# Solvatochromism and prototropism of 2-(3′-hydroxyphenyl)benzoxazole and 2-(4′-hydroxyphenyl)benzoxazole in the excited singlet state

Joy Krishna Dey and Sneh K. Dogra†
*Department of Chemistry, Indian Institute of Technology, Kanpur 208016 (India)*

(Received December 12, 1990)

**Abstract**

The absorption and fluorescence spectral properties of 2-(3′-hydroxyphenyl)benzoxazole (*m*-HPBO) and 2-(4′-hydroxyphenyl)benzoxazole (*p*-HPBO) were studied in a series of organic solvents and in aqueous solutions with $H_-/pH/H_0$ in the range 16.0 to −10.4. The Stokes shifts of *m*-HPBO and *p*-HPBO, correlated with various polarity scales, suggest that the former molecule is more polar and has a larger dipole moment than the latter in the $S_1$ state. Neutral–zwitterion and monocation–zwitterion equilibria exist in the $S_1$ state of the molecules. The excited state proton transfer reactions of *m*-HPBO were studied kinetically. The $pK_a$ values of the different prototropic equilibria in the $S_0$ and $S_1$ states were determined.

## 1. Introduction

Investigations of excited singlet state proton transfer reactions have been reported in several bifunctional molecules such as hydroxy [1, 2] and amino [3–5] derivatives of aromatic acids and heterocyclic molecules [6–13]. In the ground state of these molecules, the electron-donating groups (−OH, $-NH_2$) and the electron-withdrawing groups (−COOH, >N) behave in a similar manner to the corresponding monofunctional molecules. However, when these molecules are excited electronically, the order of ionization of the groups is reversed with respect to the normal order in the ground state because, as a result of the reorganization of electronic charge, the electron-withdrawing group becomes more basic and the electron-donating group becomes more acidic. This effect can lead to tautomerization of the molecule in which a proton migrates from the donor group to the acceptor group. If the two functional groups are ortho to each other (salicyclic acid [1] etc.) and are connected through a hydrogen bond (HB), the proton transfer occurs across the HB and the process is called intramolecular phototautomerism. The investigation of this type of molecule has recently become of interest because of their potential use as laser dyes [14]. When the two groups are widely separated (*e.g.*) β-methylumbelliferrone [15], 5-aminoindazole [7], 2-(3′-aminophenyl)benzoxazole and 2-(4′-aminophenyl)benzoxazole [12] etc.), the phototautomerism is intermolecular (*i.e.* biprotonic). The former type of phototautomerism is independent of environment, whereas the latter depends on the nature of the solvent.

†Author to whom correspondence should be addressed.

1010-6030/91/$3.50 

The present study involves two molecules, 2-(3′-hydroxyphenyl)benzoxazole (*m*-HPBO) and 2-(4′-hydroxyphenyl)benzoxazole (*p*-HPBO) which belong to the class of molecules containing widely separated donor and acceptor groups. The investigation was carried out to measure the absorption and fluorescence properties in solvents of varying polarity and hydrogen-bonding capacity, to identify the prototropic species involved in the various prototropic equilibria in the $S_0$ and $S_1$ states and to determine the dissociation constants of the prototropic equilibria in the $S_0$ and $S_1$ states.

## 2. Materials and methods

The compounds were prepared by the reaction of *o*-aminophenol with the appropriate benzoic acid derivative in polyphosphoric acid [16]; they were purified by repeated recrystallization from aqueous ethanol. The purity of the compounds was checked by the usual methods, *e.g.* thin layer chromatography (TLC), melting points and fluorescence excitation spectra. Cyclohexane (SRL), ether (Allembic), dioxane, acetonitrile (E. Merck), methanol (SDS) and dichloromethane (BDH) were purified by the procedures described in the literature [17]. Spectrograde *n*-pentane, *n*-hexane, *n*-heptane (SRL), ethylacetate (BDH), chloroform and carbon tetrachloride (SDS) were used as received. Aqueous solutions were made in tridistilled water. AnalaR grade $H_2SO_4$ (98%), NaOH and orthophosphoric acid were used as received.

Absorption spectra were recorded on a Shimadzu 190 UV spectrophotometer equipped with a 135U chart recorder. Fluorescence measurements were performed on a scanning spectrofluorometer fabricated in the laboratory [18]. A Toshniwal digital (model CL46) pH meter with a single probe glass electrode was used to measure the pH values of the aqueous solutions.

Aqueous solutions of pH in the range 4–10 were prepared by mixing appropriate amounts of NaOH and $H_3PO_4$ solutions. Hammett's modified acidity scale [19] for the $H_2SO_4$–$H_2O$ mixture and Yagil's basicity scale [20] for the NaOH–$H_2O$ mixture were employed for the preparation of solutions below pH 1.0 and above pH 13 respectively. Freshly prepared solutions were used for all measurements. The concentration of the solutions was of the order of approximately $10^{-5}$ M. Fluorescence quantum yields were determined using solutions with an optical density of less than 0.1 and quinine sulphate ($\phi = 0.55$) [21] as a reference in 0.1 N $H_2SO_4$. For fluorometric titration the solutions were excited at the isosbestic point. All fluorescence spectra reported in this work were corrected by Parker's method [22].

## 3. Results and discussion

### *3.1. Solvent effect*

The absorption and fluorescence spectra of *m*-HPBO and *p*-HPBO were studied in 13 solvents. The relevant data are given in Table 1. The absorption spectrum of *m*-HPBO is very similar to those of 2-phenylbenzoxazole (PBO) [23] and 2-(3′-methylphenyl)benzoxazole (*m*-MPBO) [24]. The spectrum is unaffected by a change in the polarity and hydrogen-bonding capacity of the solvent. The absorption spectrum of *p*-HPBO is slightly red shifted relative to that of PBO and the red shift increases as the polarity of the solvent is increased; in methanol and water the spectrum is slightly blue shifted.

TABLE 1

Absorption ($\lambda_a$) and fluorescence ($\lambda_f$) band maxima (nm), log $\epsilon_{max}$ and fluorescence quantum yields ($\phi_f$) of *m*-HPBO and *p*-HPBO in various solvents and at various acid concentrations

| Solvent | *m*-HPBO | | *p*-HPBO | |
|---|---|---|---|---|
| | $\lambda_a$(log $\epsilon_{max}$) | $\lambda_f(\phi_f)$ | $\lambda_a$(log $\epsilon_{max}$) | $\lambda_f(\phi_f)$ |
| *n*-Pentane | 295[b] | 320 | 297 | 317 |
| | 316(s) | 335(0.17) | 302 | 335(0.72) |
| | | 350 | 317(s) | 352 |
| | | 370 | | 365 |
| *n*-Hexane | 295[b] | 320 | 297 | 320 |
| | 316(s) | 335(0.58) | 303 | 340(0.52) |
| | | 352 | 318(s) | 355 |
| | | 365 | | 365 |
| *n*-Heptane | 295[b] | 320 | 295 | 320 |
| | 300 | 335(0.76) | 301 | 338(0.54) |
| | 316(s) | 352 | 315(s) | 355 |
| | | 370 | | 365 |
| Cyclohexane | 295[b] | 320 | 296 | 325 |
| | 317(s) | 335(0.65) | 302 | 340(0.35) |
| | | 352 | 315(s) | 355 |
| | | 370 | | |
| Ether | 298(4.35) | 345(0.68) | 299(4.52) | 325 |
| | 317(s) | | 305(4.54) | 342(0.59) |
| | | | 318(s) | 360 |
| | | | | 370 |
| Dioxane | 296(4.36) | 350(0.75) | 298(4.51) | 327(0.51) |
| | 319(s) | | 305(4.53) | 345 |
| | | | 320(s) | 360 |
| Ethylacetate | 298(4.35) | 355(0.72) | 297(4.52) | 330 |
| | 317(s) | | 305(4.54) | 345(0.53) |
| | | | 317(s) | 360 |
| Acetonitrile | 295(4.34) | 360(0.66) | 297(4.57) | 330(0.55) |
| | 317(s) | | 304(4.59) | 345 |
| | | | 317 | 360 |
| Methanol | 296(4.31) | 370(0.27) | 304(4.54) | 335(0.52) |
| | 316(s) | | – | 350 |
| | | | | 365 |
| Water | 291 | | | |
| | 297(4.36) | 390(0.18) | 301(4.58) | 360(0.2) |
| | 315(s) | | – | |

(*continued*)

TABLE 1. (*continued*)

| Solvent | *m*-HPBO | | *p*-HPBO | |
|---|---|---|---|---|
| | $\lambda_a$(log $\epsilon_{max}$) | $\lambda_f(\phi_f)$ | $\lambda_a$(log $\epsilon_{max}$) | $\lambda_f(\phi_f)$ |
| $CH_2Cl_2$ | 297(4.36) | 330(0.66) | 298(4.57) | 325(0.49) |
| | 302 | 340 | 304(4.59) | 345 |
| | 316(s) | 360 | | 360 |
| | | 370 | | 370 |
| $CHCl_3$ | 299 | 360(0.17) | 299 | 335(0.13) |
| | 319(s) | | 305 | 355 |
| | | | 319 | |
| $CCl_4$ | 298 | 323(0.1) | 298 | 325(0.03) |
| | 305 | 340 | 304 | 345 |
| | 319(s) | 360 | 318 | 358 |
| | | 380 | | 370 |
| Monoanion (pH 12) | 295(4.35) 333(s) | 400(0.06) | 330(4.63) | 395(0.21) |
| Neutral (pH 4) | 297(4.36) 315(s) | 370(0.03)[a] | 302(4.58) | 360(0.2) |
| Monocation ($H_0$ −1.5) | 309(4.36) | 410(0.09) | 327(4.59) | 390(0.91) |
| ($H_0$ −10) | 315 | 397 | 322 | 390 |

s, Shoulder.
[a]Measured at pH 2.5.
[b]Saturated solution.

The fluorescence spectrum of *m*-HPBO is structured in non-polar solvents but the structure disappears in polar and protic solvents. In *p*-HPBO the structure in the fluorescence spectrum in retained even in methanol and water. The fluorescence spectra of both *m*-HPBO and *p*-HPBO are red shifted with an increase in solvent polarity. The red shift is greater for *m*-HPBO than for *p*-HPBO. The fluorescence quantum yield of *p*-HPBO remains constant in all solvents except water. The same is true of *m*-HPBO, with the exception of methanol and water. The fluorescence quantum yield in chlorinated solvents decreases with an increase in the number of chlorine atoms.

A previous investigation of PBO [24] has suggested that the long wavelength transition is localized on the phenyl ring and is $\pi \rightarrow \pi^*$ in nature. The moment corresponding to this transition is polarized along the long axis. Since the band shape and the positions of the band maxima of *p*-HPBO and *m*-HPBO are similar to those of PBO, the same conclusion can also be drawn for these molecules. The vibrational frequency (approximately $1400 \pm 50$ cm$^{-1}$), calculated from the structured fluorescence spectra of *p*-HPBO and *m*-HPBO, is similar to that obtained from the fluorescence spectrum of PBO and confirms our conclusion that the emitting state ($\pi$, $\pi^*$) in these molecules is the same. The red shifts in the absorption and fluorescence spectra of *p*-HPBO relative to those of *m*-HPBO can be explained by the resonance effect of

the −OH group which extends the conjugation leading to structure II′. Structure II′ is more rigid than *m*-HPBO and, being polar, is more stable in polar solvents. As a result, the fluorescence spectrum of *p*-HPBO is structured and red shifted even in polar solvents. Similar features have also been observed in 2-(4′-aminophenyl)-benzimidazole [25], 2-(4′-hydroxyphenyl)benzimidazole [26], 2-(4′-aminophenyl)-benzoxazole [12], 2-(4′-hydroxyphenyl)benzothiazole and 2-(4′-aminophenyl)benzo-thiazole [27].

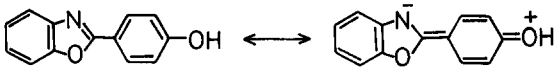

II II′

*3.2. Correlation of Stokes shift with polarity parameters*

The Stokes shift can be related to solvent polarity by the Lippert equation [28]

$$\Delta\bar{\nu}_{ss} = \frac{2(\mu_e - \mu_g)^2}{hca^3} f(D,n) + K \tag{1}$$

where

$$f(D,n) = \frac{D-1}{2D+1} - \frac{n^2-1}{2n^2+1} \tag{2}$$

or

$$f(D,n) = \frac{(D-1)/(2D+1) - (n^2-1)/(2n^2+1)}{\{1-\beta(n^2-1)/(2n^2+2)\}^2\{1-\beta(D-1)/(2D+2)\}} \tag{3}$$

$\Delta\bar{\nu}_{ss}$ is the Stokes shift ($cm^{-1}$), $\mu_g$ and $\mu_e$ are the dipole moments of the fluorophore in the ground and excited states respectively, $c$ is the velocity of light, $h$ is Planck's constant, $K$ is a constant, $D$ and $n$ are the static dielectric constant and refractive index of the solvent respectively and $\beta$ is a constant factor (in most cases, approximately unity).

The Stokes shifts of *m*-HPBO and *p*-HPBO measured in different solvents were correlated with the Onsager $f(D,n)$ [29], Bilot–Kawski (BK) [30] and Reichardt–Dimroth ($E_T(30)$) [31] parameters (Table 2). The Onsager and BK parameters are defined by eqns. (2) and (3) respectively, and $E_T(30)$ is an empirical scale based on the spectral shifts of *N*-phenolbetaine dye in solvents of varying polarity.

Figures 1(a) and 1(b) show the plots of $\Delta\bar{\nu}_{ss}$ *vs.* the BK and $f(D,n)$ parameters. It can be seen that, with the exception of $CHCl_3$, $CCl_4$ and hydroxylic solvents, the plots are linear; this suggests that the solute–solvent interactions are not very large and that general interactions play a major role in the spectral characteristics of these compounds. The large deviations in hydroxylic solvents can be explained as follows. It is well established that the −OH group becomes more acidic in the $S_1$ state and thus can donate a proton easily to the solvent; in contrast in the $S_0$ state the −OH group acts as a proton acceptor. This means that the hydrogen bond between the solvent molecule and the lone pair of the −OH group in the $S_0$ state is broken on excitation and a hydrogen bond is formed between the proton of the −OH group and the lone pair of the solvent molecule. As a result, large Stokes shifts are observed in the fluorescence spectra of both molecules in polar and protic solvents.

The deviation in the case of $CHCl_3$ and $CCl_4$ can be explained as follows. It is well established that the fluorescence of fluorophores is quenched by $CHCl_3$ and $CCl_4$

TABLE 2

Stokes shifts and polarity parameters

| Solvent | $\Delta f$[a] | BK[b] | $E_T(30)$[c] (kJ mol$^{-1}$) | $\Delta\bar{\nu}_{ss} \times 10^{-3}$ (cm$^{-1}$) | |
|---|---|---|---|---|---|
| | | | | *m*-HPBO | *p*-HPBO |
| *n*-Pentane | | | | 4.05 | 3.26 |
| *n*-Hexane | 0.002 | 0.002 | 129.3 | 4.05 | 3.59 |
| *n*-Heptane | 0.001 | 0.001 | 130.0 | 4.05 | 3.64 |
| Cyclohexane | −0.001 | −0.001 | 130.5 | 4.05 | 3.70 |
| Ether | 0.167 | 0.365 | 144.8 | 4.57 | 3.55 |
| Dioxane | 0.02 | 0.043 | 150.6 | 4.87 | 3.80 |
| Ethylacetate | 0.201 | 0.488 | 159.4 | 5.39 | 3.80 |
| Acetonitrile | 0.305 | 0.864 | 192.4 | 6.12 | 3.91 |
| Methanol | 0.309 | 0.858 | 232.2 | 6.76 | 4.32 |
| Water | 0.32 | 0.924 | 264.0 | 8.72 | 5.45 |
| $CH_2Cl_2$ | 0.218 | 0.586 | 172.0 | 5.89 | 3.91 |
| $CHCl_3$ | 0.149 | 0.372 | 163.6 | 5.67 | 4.62 |
| $CCl_4$ | 0.218 | 0.586 | 172.0 | 5.89 | 4.96 |

[a]Values calculated according to eqn. (2), using the values of $D$ and $n$ from ref. 17.
[b]Most of the values are taken from ref. 32; others are calculated with the $D$ and $n$ values taken from ref. 17.
[c]From ref. 31.

[32]. Since the energy transfer from the excited fluorophore to the quencher molecule is endothermic and no evidence of complex formation in the ground state is observed when the absorption spectra are measured in cyclohexane at various concentrations of $CHCl_3$ or $CCl_4$, the fluorescence quenching can be explained by the formation of a charge transfer complex between the fluorophore and the quencher molecules in the $S_1$ state. The rate of formation of the charge transfer complex between a given fluorophore and quencher increases with an increase in the electron affinity of the quencher. This is demonstrated by the observation that the fluorescence quantum yield decreases on going from $CH_2Cl_2$ to $CCl_4$.

The plots of $\Delta\bar{\nu}_{ss}$ *vs.* $E_T(30)$ are given in Fig. 1(c). As expected, these plots are more linear, because the $E_T(30)$ value includes both general solvent effects and hydrogen-bonding effects. However, as there is no contribution from the solute–solvent charge transfer interactions to the $E_T(30)$ value, a non-linearity is observed for $CHCl_3$ and $CCl_4$. The deviation of the Stokes shift for *m*-HPBO in water is due to the presence of a monoanion species (see later) in addition to the neutral species.

*3.3. Excited state dipole moment*

The difference between the excited state and ground state dipole moments ($\mu_e - \mu_g$) was calculated from the plots of $\Delta\bar{\nu}_{ss}$ *vs.* $f(D, n)$ or BK values as suggested by eqn. (1). The accuracy of the results is limited by the value of $a$ which has been taken as 5.0 Å for both molecules. The values of $\mu_e - \mu_g$ obtained for *m*-HPBO from the plots of Fig. 1(b) and 1(a) are 1.76 D and 0.86 D respectively. The corresponding values for *p*-HPBO are 1.3 D and 0.45 D. This shows that the dipole moment increases on excitation and this increase is larger for *m*-HPBO. Since the value of $\mu_g$ is not known we were unable to calculate the $\mu_e$ value.

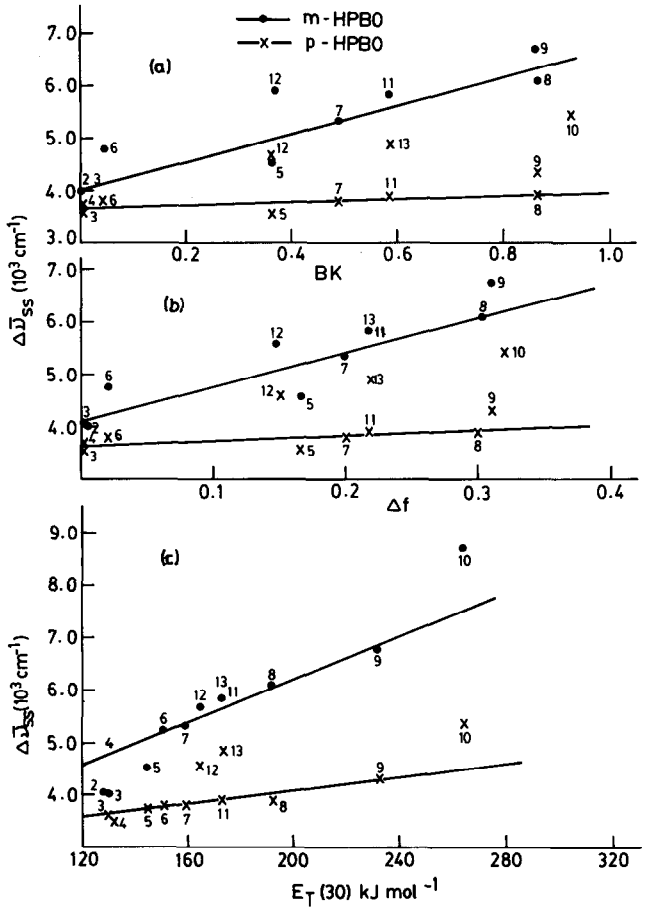


Fig. 1. Plot of Stokes shift ($\Delta\bar{\nu}_{ss}$) *vs.* BK parameter (a), $f(D, n)$ (b) and $E_T(30)$ (c).

### *3.4. Effect of acid concentration*

The spectral characteristics and prototropic equilibria in the $S_0$ and $S_1$ states of the molecules were studied in the $H_-/pH/H_0$ range 16 to $-10.4$. The relevant data are given in Table 1. The possible prototropic equilibria involved in the molecules can be represented as

$$^+HAOH_2^+ \rightleftharpoons {}^+HAOH + H^+ \quad (4)$$

$$^+HAOH \rightleftharpoons AOH + H^+ \quad (5)$$

$$AOH \rightleftharpoons AO^- + H^+ \quad (6)$$

where $^+HAOH_2^+$, $^+HAOH$, AOH and $AO^-$ represent the dication, monocation, neutral and monoanion forms respectively. The $pK_a$ values (Table 3) for the above equilibria in the $S_0$ state were determined from the absorption spectral data and those in the $S_1$ state were determined by fluorometric titration and Forster cycle methods. The behaviour of the prototropic equilibria is similar for both molecules in the $S_0$ state but different in the $S_1$ state. Therefore the results are discussed together for the ground state but separately for the excited singlet state.

TABLE 3

Ground state ($S_0$) and excited state ($S_1$) dissociation constants of various prototropic reactions of *p*-HPBO and *m*-HPBO

| Equilibrium | $pK_a$ | $pK_a^*$ | | |
|---|---|---|---|---|
| | | FT | FC | |
| | | | Abs | Flu |
| *m*-HPBO | | | | |
| Monocation ⇌ neutral | −0.2 | – | – | – |
| Neutral ⇌ Monoanion | 9.9 | 3.5 | 6.3 | 5.6 |
| Zwitterion ⇌ neutral | – | 1.0 | | |
| Monocation ⇌ zwitterion | – | −1.2 | | |
| *p*-HPBO | | | | |
| Monocation ⇌ neutral | 0.5 | – | – | – |
| Neutral ⇌ monoanion | 8.8 | – | 2.9 | 3.6 |
| Zwitterion ⇌ neutral | – | 1.5 | – | – |
| Monocation ⇌ zwitterion | – | −1.8 | – | – |

FT, fluorometric titration method; FC, Forster cycle method.

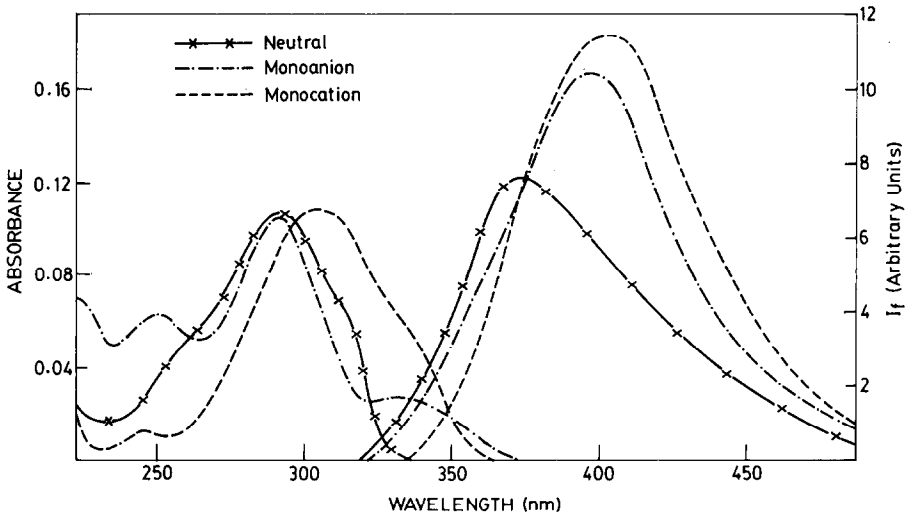


Fig. 2. Absorption and fluorescence spectra of the prototropic species of *m*-HPBO.

*3.4.1. Ground state*

The molecules are present as monoanions in the higher pH range (pH ⩾ 10), in neutral form in the pH range 1.0–7, as monocations in the $H_0$ range −1.0 to −9.0, and as dications below $H_0$ −10.4. These assignments are based on the spectral shifts observed for the molecules in the above acidity range and the spectral characteristics of similar systems reported in the literature [12, 26, 27]. The absorption spectra of the different species of the molecules are shown in Figs. 2 and 3. As expected, the monoanion is formed by deprotonation of the −OH group, the monocation by protonation

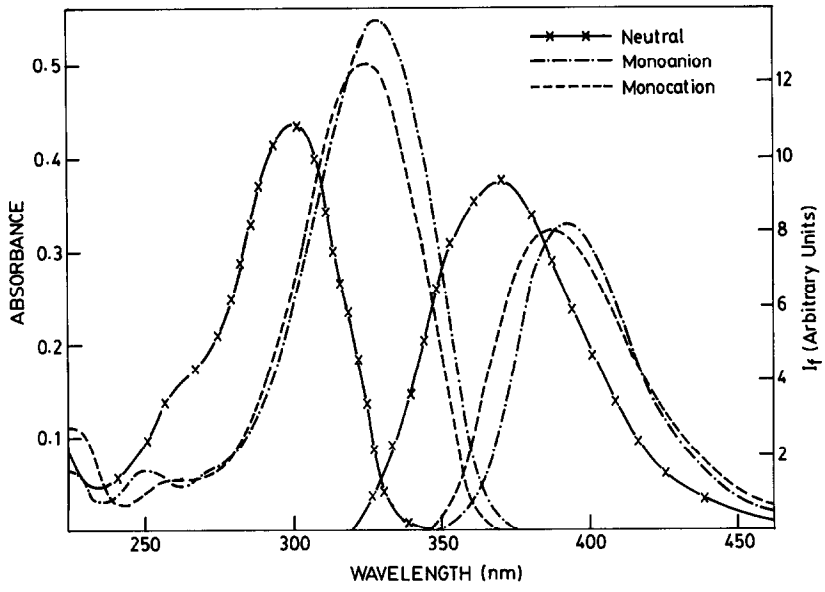


Fig. 3. Absorption and fluorescence spectra of the prototropic species of *p*-HPBO.

at the ring nitrogen atom and the dication by a second protonation of the hydroxylic oxygen.

The p$K_a$ values (Table 3) of equilibria (6) and (5) (p$K_a$(6), 8.8(*p*-HPBO); 9.9(*m*-HPBO); p$K_a$(5), 0.5(*p*-HPBO); −0.2(*m*-HPBO)) can be explained by the resonance effect of the −OH group as discussed earlier. As a result of this effect the −OH proton becomes more acidic and the ring nitrogen becomes more basic.

*3.4.2. Excited singlet state ($S_1$)*

The effect of acid concentration on the prototropic equilibria of the molecules in the first excited singlet state ($S_1$) was studied by measuring their steady state fluorescence properties at various acid or base concentrations. The relevant data are given in Table 1. The prototropic equilibria in the pH/$H_0$ range 4 to −6 in the $S_1$ state of the molecules are different from the corresponding ground state equilibria. The fluorescence spectral characteristics of *m*-HPBO in the high pH region are different from those of *p*-HPBO.

*3.4.2.1. 2-(3'-Hydroxyphenyl)benzoxazole.* The fluorescence spectrum of this molecule is very broad in aqueous solutions in the pH range 5–9; the intensity remains constant in this pH range. With an increase in pH above 9, the intensity first increases to pH 11 ($\lambda_{max}$ = 400 nm) and then decreases; no new bands are apparent. The bandwidth at half-maximum height (BWHM) also decreases to pH 11 and then remains constant. With a decrease in pH below 4, the intensity and BWHM decrease, accompanied by a shift in the fluorescence maximum from 400 to 370 nm at pH 2. The intensity of the blue-shifted band also decreases; no new bands are observed with a further increase in $H^+$ ion concentration. A new fluorescence band at approximately 410 nm starts to appear at an acid concentration of greater than 0.3 M. The increase in intensity is slow to $H_0$ −3, but below $H_0$ −3 the increase is very rapid and continues to $H_0$

$-9$. No change is observed in the band maximum or BWHM in the acidity range $H_0$ $-3$ to $H_0$ $-9$. A blue-shifted band ($\lambda_{max}=397$ nm) with lower intensity is observed at $H_0$ $-10.4$.

The fluorescence excitation spectra in solutions of pH 12 and 2 resemble the absorption spectra of the monoanion and neutral species respectively. Therefore the fluorescence bands at 400 and 370 nm can be assigned to the monoanion and neutral forms respectively. The broadness of the fluorescence spectrum in the pH range 5–9 is due to the coexistence of the monoanion and neutral molecules. Since, in this pH region, *m*-HPBO is present only in the neutral form in the $S_0$ state, the monoanion observed in the $S_1$ state must be formed on excitation, in agreement with the earlier results [33] that the hydroxyl group becomes strongly acidic in the $S_1$ state. Similarly, based on earlier results [33], the red-shifted fluorescence band at 410 nm can be assigned to the monocation, formed by protonation of the tertiary nitrogen atom. The fluorescence spectra of the various prototropic species are depicted in Fig. 2.

The $pK_a^*$ values of these prototropic equilibria were determined using fluorometric titration. The calculation of the relative fluorescence intensities for the neutral form ($I/I_0$) and the monoanion ($I'/I_0'$) was difficult because the fluorescence intensity of the neutral form does not remain constant over any pH range. This is because other prototropic reactions involving the neutral form occur simultaneously in the pH range 0.0–3 in the $S_1$ state. Such problems were not encountered for the monoanion and monocation because these species are present exclusively at the extreme conditions of base or acid concentration. Since the fluorescence intensity of the neutral form of *p*-HPBO starts to decrease at pH 3 to form a zwitterion in the $S_1$ state (see below) and the $pK_a$ value of the monocation–neutral equilibrium of *p*-HPBO is one $pK_a$ unit more than that of *m*-HPBO, it can be assumed that the fluorescence intensity of the neutral form of *m*-HPBO will be at its maximum around pH 3. On the basis of this assumption, the relative fluorescence intensities of the neutral ($I/I_0$) and monoanion ($I'/I_0'$) forms were determined experimentally from the fluorescence spectra using the method of Weller [34]. The values of the relative fluorescence intensities of these two forms are plotted in Fig. 4 as a function of pH. Stretched sigmoidal curves are obtained with two inflexion points, one of which corresponds to $pK_a$ (9.9) and the other to

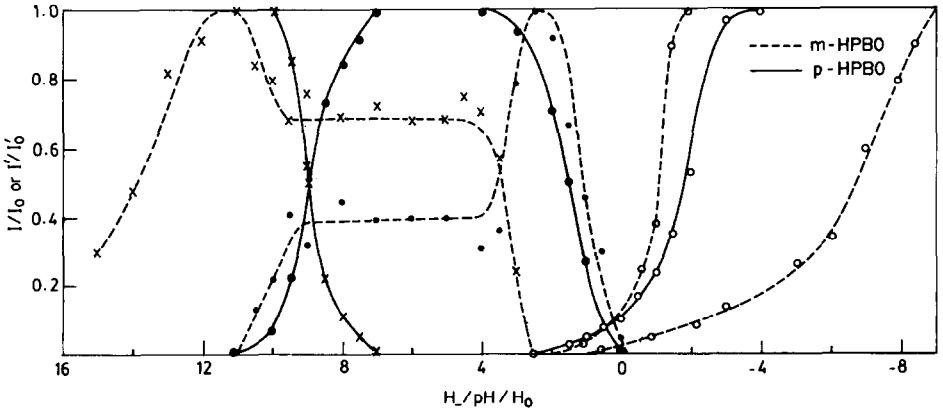


Fig. 4. Plot of the relative fluorescence intensities ($I/I_0$ or $I'/I_0'$) *vs.* pH/$H_0$: monoanion (x); neutral (●); monocation (○).

p$K_a$* (3.5). This does not provide an accurate value but the error will not be more than one p$K_a$ unit. Even though the point with $I/I_0 = I'/I'_0 \approx 0.5$ occurs at 3.5, the extension of the curves to pH 12 shows that the equilibrium in the excited state is not complete. This type of behaviour indicates that the rate of the proton transfer reaction in the $S_1$ state is comparable with the rate of fluorescence decay. The shapes of the fluorometric titration curves obtained can be explained on the basis of the kinetics of the excited state proton transfer, as discussed for 1- and 2-naphthols [35] and 9-phenanthrol [36]. Writing reaction (6) in the following detailed form

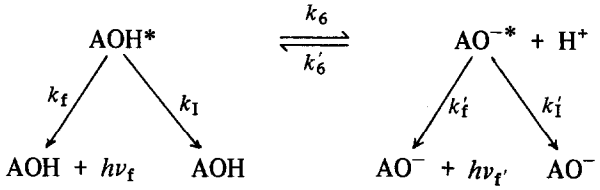


and using simple steady state approximation, the relative fluorescence intensities of *m*-HPBO ($I/I_0$) and its monoanion ($I'/I'_0$) can be written as

$$\frac{I}{I_0} = \frac{1+k'_6\tau'_0[H^+]}{1+k_6\tau_0+k'_6\tau'_0[H^+]} \tag{7}$$

$$\frac{I'}{I'_0} = \frac{k_6\tau_0}{1+k_6\tau_0+k'_6\tau'_0[H^+]} \tag{8}$$

where $k_6$ is the pseudo-first-order rate constant for proton transfer from the excited *m*-HPBO molecule, $k_f$ and $k_I$ are the rate constants of fluorescence and radiationless decay of the excited molecule and the primed values are similar terms for the excited monoanion. The plateau in the pH range 4–9 arises because the rate of reaction with the solvent molecules in eqn. (6) is comparable with or greater than the rate of fluorescence of *m*-HPBO, and the rate of second-order protonation of the monoanion is much less than the rate of fluorescence. Under these conditions, eqns. (7) and (8) reduce to

$$\frac{I}{I_0} = \frac{1}{1+k_6\tau_0} \tag{9}$$

$$\frac{I'}{I'_0} = \frac{k_6\tau_0}{1+k_6\tau_0} \tag{10}$$

Equations (9) and (10) clearly indicate that $I/I_0$ and $I'/I'_0$ are independent of $[H^+]$ or $[OH^-]$ and thus a plot of $I/I_0$ or $I'/I'_0$ *vs.* pH should be parallel to the pH axis. The plots of Fig. 4 confirm this. The values of $I/I_0$ and $I'/I'_0$ obtained from the flat regions of the curves are 0.39 and 0.69 respectively. Using eqns. (9) and (10), the values of $k_6\tau_0$ are 1.56 and 2.2 respectively, giving a mean of 1.89. The difference between the values of $k_6\tau_0$, calculated using eqns. (9) and (10), is due to the assumption made earlier in the calculation of the $I_0$ value of the neutral species. This also leads to $I/I_0 + I'/I'_0 = 1.08$ in the plateau region, whereas $I/I_0 + I'/I'_0$ should be equal to unity.

Expression (11) is obtained by dividing eqn. (7) by eqn. (8)

$$\frac{II'_0}{I_0I'} = \frac{1}{k_6\tau_0} + \frac{k'_6\tau'_0}{k_6\tau_0}[H^+] \tag{11}$$

A plot of the ratio of the experimentally determined fluorescence intensities *vs.* $[H^+]$ should give a straight line with a slope equal to $k'_6\tau'_0/k_6\tau_0$ and an intercept of $1/k_6\tau_0$.

Figure 5 shows that this plot is linear in the pH range 3.0–4. A deviation from linearity at pH < 3 may be due to other reactions of the neutral *m*-HPBO species as mentioned earlier. The values of $k_6\tau_0$ and $k'_6\tau'_0$ obtained from the linear portion of the curve are 2.4 $dm^3\ mol^{-1}$ and $4.5\times10^3\ dm^3\ mol^{-1}$ respectively. The value of $k_6\tau_0$ obtained from this plot is similar to that obtained from the plateau. Knowing the lifetimes $\tau_0$ and $\tau'_0$, we can calculate the respective rate constants $k_6$ and $k'_6$ and thereby the $pK_a^*(6)$ value.

The Forster cycle method [37] cannot be used to calculate the $pK_a^*(4)$ and $pK_a^*(5)$ values for the dication–monocation and monocation–neutral equilibria, because the $pK_a(4)$ value is not known and equilibrium (5) is different. The $pK_a^*(6)$ values obtained for the neutral–monoanion equilibrium from the Forster cycle method, using absorption and fluorescence data, are 6.3 and 5.6 respectively. The disagreement between the values may be due to the use of $\tilde{\nu}_{max}$ instead of $\tilde{\nu}_{0-0}$ for the 0–0 transition (especially in the absorption spectrum of the anion) and the different solvent relaxations of the conjugate acid–base pairs in the ground and excited singlet states. This is further demonstrated by the large solvent effect on the fluorescence spectrum of neutral *m*-HPBO. A more accurate value can be determined if the lifetimes of the conjugate acid–base pairs are known.

It can be seen in Fig. 4 that no correlation is observed between the decrease in the fluorescence intensity of the neutral species and the increase in the fluorescence intensity of the monocation. This may be due to the proton-induced fluorescence quenching of the neutral species or to the formation of a non-fluorescent species (most probably a zwitterion). This is an excited state phenomenon because the neutral

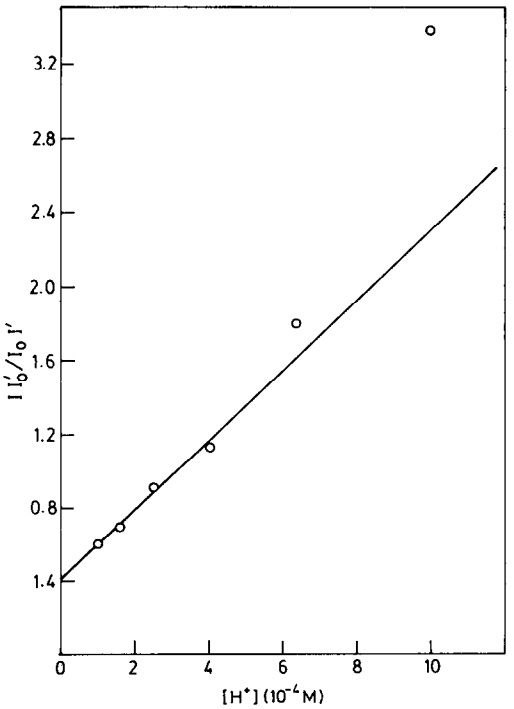


Fig. 5. Plot of the ratio of the relative intensities ($II'_0/I_0I'$) *vs.* hydrogen ion concentration [$H^+$].

species is present in the $S_0$ state up to an $H^+$ ion concentration of 0.1 M (pH 1). The former explanation can be rejected for the following reason. The $pK_a^*$ value for any prototropic equilibrium can be determined from the formation curve of the species. If it is assumed that there are only two prototropic species in the $S_1$ state (neutral and monocation) and the decrease in the fluorescence intensity of the neutral species is due to proton-induced quenching, the formation curve of the monocation gives $pK_a^*(5) = -1.9$. This indicates that the tertiary nitrogen atom becomes more acidic or less basic in the $S_1$ state, in contrast with established results. The formation of the zwitterion in the $S_1$ state occurs via biprotonic (intermolecular) phototautomerization and thus will depend on the nature of the environment. Although at pH 5–8, the protonation and deprotonation reaction rates are very slow compared with radiative decay, it is possible that at pH 1–2, the rates of deprotonation of the $-OH$ group and protonation of the tertiary nitrogen atom are comparable with the radiative decay rates leading to the formation of a zwitterion. Because of the non-fluorescent nature of the zwitterion, it is difficult to find the ground state precursor, but it seems to be a neutral species. As mentioned earlier, $pK_a(5) = -0.2$, and thus the concentration of the monocation in the $S_0$ state will be negligible at $pH > 1.2$, whereas the fluorescence intensity of the neutral species starts to decrease below pH 3. The above discussion indicates that the following prototropic reactions will occur in the $S_1$ state of *m*-HPBO (dissociation constants of $-1.2$ and 1.0 respectively)

$$^+HAOH^* \rightleftharpoons {}^+HAO^{-*} + H^+$$

$$^+HAO^{-*} \rightleftharpoons AOH^*$$

A similar behaviour has also been observed in 2-(hydroxyphenyl)benzothiazoles, 2-(aminophenyl)benzoxazoles [12] and 2-(aminophenyl)benzothiazoles [27].

Finally the increase in the fluorescence intensity of the monocation, with no change in the band maximum and BWHM below $H_0 -3$, is due to the change in the solvent structure. At low acid strength, a large number of water molecules are present; the number decreases with an increase in acid concentration. At high acid concentration, the water molecules will only be involved in the solvation of the ionic species produced by sulphuric acid, rather than in the solvation of the monocations of *m*-HPBO; this will lead to a decrease in the rates of the radiationless processes which occur due to solvation. The increase in the viscosity of the medium with an increase in acid concentration may also increase the fluorescence quantum yield of the fluorophore, but the former seems to be more probable.

*3.4.2.2. 2-(4'-Hydroxyphenyl)benzoxazole.* In the ground state, the molecule is present as the monoanion above pH 10.0, the neutral form in the pH range 2.0–8.0, the monocation at $H_0$ below $-1.0$ and the dication at $H_0 < -9.0$. The absorption and fluorescence spectra of the prototropic species are given in Fig. 3. The prototropic equilibrium in the $S_1$ state above pH 7.0 is similar to that in the $S_0$ state. Below pH 3.0 the fluorescence intensity of the neutral molecule decreases, accompanied by a slow increase in the monocation band. The intensity of the monocation band continues to increase to $H_0 -4.0$, but the neutral band decreases to zero intensity at pH 0.5. Thus, there is no correlation between the decay and formation curves of these species (see Fig. 4). No change in the BWHM of the monocation band is observed in this acidity region. These features are similar to those of *m*-HPBO and thus can be explained, in the same way, by the formation of a non-fluorescent zwitterion in the $S_1$ state. The only difference is that the rate of formation of the zwitterion is slower in this case.

The $pK_a^*$ value (calculated by the Forster cycle method) for reaction (6) indicates that the $-OH$ group becomes more acidic in the $S_1$ state. Fluorometric titration gives the ground state $pK_a$ value, indicating non-establishment of the equilibrium in the $S_1$ state. The $pK_a^*$ values of the excited state equilibria are given in Table 3.

## 4. Conclusions

The following conclusions can be drawn from this study.

(i) The resonance effect of the $-OH$ group makes *p*-HPBO more rigid than *m*-HPBO as indicated by the structured fluorescence spectra in solvents except water and the lower and higher $pK_a$ values of the neutral–monoanion and monocation–neutral equilibria compared with the values for *m*-HPBO.

(ii) *m*-HPBO is more polar in the $S_1$ state than in the $S_0$ state. The increase in the dipole moment of *m*-HPBO on excitation is greater than that of *p*-HPBO.

(iii) The stretched sigmoidal-type fluorometric titration curves for the neutral–monoanion equilibrium of *m*-HPBO indicate that the lifetimes of the conjugate acid and base are comparable with the reciprocal rate constants of the protonation and deprotonation reactions. However, in the case of *p*-HPBO, the fluorescence decay rates are faster than the rates of the protonation and deprotonation reactions.

(iv) The lack of correlation between the decrease in the fluorescence intensity of the neutral molecule and the increase in the fluorescence intensity of the monocation of both *m*- and *p*-HPBO lead us to propose the formation of a non-fluorescent zwitterion in the $S_1$ state. The zwitterion is formed as a result of biprotonic phototautomerism.

## References


1 P. J. Kovi, C. L. Miller and S. G. Schulman, *Anal. Chim. Acta, 61* (1972) 7.
2 P. J. Kovi and S. G. Schulman, *Anal. Chim. Acta, 67* (1973) 259.
3 S. Srivastava and S. K. Dogra, *J. Photochem., Photobiol. A: Chem., 46* (1989) 329.
4 A. Tramer, *J. Phys. Chem., 74* (1970) 887.
5 D. W. Ellis and L. B. Rogers, *Spectrochim. Acta, 20* (1964) 1709.
6 B. Zalis, A. C. Capomacchia, D. Jackson and S. G. Schulman, *Talanta, 20* (1973) 33.
7 M. Swaminathan and S. K. Dogra, *J. Am. Chem. Soc., 105* (1983) 6223.
8 A. K. Mishra and S. K. Dogra, *Indian J. Chem. A, 24* (1985) 364.
P. Phaniraj, A. K. Mishra and S. K. Dogra, *Indian J. Chem. A, 24* (1985) 913.
9 A. K. Mishra and S. K. Dogra, *J. Photochem., 31* (1985) 333.
10 H. K. Sinha and S. K. Dogra, *Chem. Phys., 102* (1986) 337.
11 J. Durmis, M. Karvas and Z. Manasek, *Collect. Czech. Chem. Commun., 38* (1973) 215.
O. I. Betin, R. N. Nurumukhametov, D. N. Shigonon and N. L. Chernova, *Dokl. Akad. Nauk SSSR, 227* (1976) 126.
D. L. Williams and A. Heller, *J. Phys. Chem., 74* (1970) 4473.
A. Mordzinski and A. Grabowska, *Chem. Phys. Lett., 90* (1983) 122.
G. J. Woolfe, M. Melzig, S. Schneider and F. Dorr, *Chem. Phys., 77* (1983) 213.
M. Krishnamurthy and S. K. Dogra, *J. Photochem., 32* (1986) 235.
12 J. K. Dey and S. K. Dogra, *Chem. Phys., 143* (1990) 97.
13 H. K. Sinha and S. K. Dogra, *Bull. Chem. Soc. Jpn., 62* (1989) 2668.
H. K. Sinha and S. K. Dogra, *Spectrochim. Acta, Part A, 45* (1989) 1289.
14 P. Sengupta and M. Kasha, *Chem. Phys. Lett., 68* (1979) 382.
A. U. Khan and M. Kasha, *Proc. Natl. Acad. Sci. U.S.A, 80* (1983) 1767.
D. A. Parthenopoutos and M. Kasha, *Chem. Phys. Lett., 146* (1988) 77.

P. Chou, D. McMarrow, T. J. Aartsma and M. Kasha, *J. Phys. Chem., 88* (1984) 459.
A. U. Acuna, F. Mat, J. Catalan, J. M. Figuere and J. M. Munez, *Chem. Phys. Lett., 132* (1986) 567.
A. U. Acuna, A. Costela and J. M. Munoz, *J. Phys. Chem., 90* (1986) 2807.
15 G. J. Yakatan, R. J. Junean and S. G. Schulman, *Anal. Chem., 44* (1972) 1044.
16 D. W. Hein, R. J. Alheim and J. J. Leavitt, *J. Am. Chem. Soc., 79* (1957) 427.
17 J. A. Riddick and W. B. Bunger, *Organic Solvents,* Wiley-Interscience, New York, 1970, pp. 592–594, 798–805.
18 M. Swaminathan and S. K. Dogra, *Indian J. Chem. A, 22* (1983) 853.
19 M. J. Jorgenson and D. R. Hartler, *J. Am. Chem. Soc., 85* (1963) 878.
20 G. Yagil, *J. Phys. Chem., 71* (1967) 1034.
21 G. G. Guilbault, *Practical Fluorescence,* Dekker, New York, 1971, p. 13.
22 C. A. Parker, *Photoluminescence of Solutions with Applications to Photochemistry and Analytical Chemistry,* Elsevier, Amsterdam, 1962, p. 153.
23 R. Passerini, *J. Chem. Soc.,* (1954) 2256.
24 J. K. Dey and S. K. Dogra, *Indian J. Chem., 29A* (1990) 1153 and references cited therein.
25 A. K. Mishra and S. K. Dogra, *Bull. Chem. Soc. Jpn., 58* (1985) 3587.
26 H. K. Sinha and S. K. Dogra, *J. Photochem. Photobiol. A: Chem., 36* (1987) 149.
27 J. K. Dey and S. K. Dogra, *Can J. Chem.,* in the press.
J. K. Dey and S. K. Dogra, *Bull. Chem. Soc. Jpn.,* in the press
28 E. Lippert, *Z. Naturforsch., 10* (1955) 541.
29 E. Lippert, *Z. Naturforsch., Teil A, 17* (1962) 621.
N. Mataga Y. Kaifu and M. Koizumi, *Bull. Chem. Soc. Jpn., 28* (1955) 690.
30 P. Supan, *J. Chem. Soc. A,* (1986) 3125.
31 K. Dimroth, C. Reichardt, T. Siepmann and F. Bohlmann, *Liebigs Ann. Chem., 661* (1963) 1.
C. Reichardt, *Angew. Chem. Int. Ed. Engl., 18* (1979) 98.
32 R. O. Loutfy and A. C. Somersall, *Can. J. Chem., 54* (1976) 76.
G. E. Johnson, *J. Phys. Chem., 84* (1980) 2940.
T. Takahasi, K. Kikuchi and H. Kokubun, *J. Photochem., 14* (1980) 67.
W. R. Ware and C. Lewis, *J. Chem. Phys., 57* (1972) 3546.
D. Saperstein and E. Levine, *J. Chem. Phys., 62* (1975) 356.
33 J. F. Ireland and P. A. H. Wyatt, *Adv. Phys. Org. Chem., 12* (1976) 131.
34 A. Weller, *Z. Phys. Chem. (N.F.), 17* (1958) 224.
35 C. M. Harris and B. K. Sellinger, *J. Phys. Chem., 84* (1980) 891, 1366, and references cited therein.
36 M. Swaminathan and S. K. Dogra, *J. Chem. Soc., Perkin Trans. 2,* (1984) 947.
37 Th. Forster, *Z. Elektrochem. Angew. Phys. Chem., 54* (1950) 42, 531.